



# Effects of friction stir welding parameters on the mechanical properties of AA7075-T6

**Duong Dinh Hao\*, Tran Hung Tra**

Department of Engineering Mechanics, Nha Trang University,  
02 Nguyen Dinh Chieu Street, Nha Trang City, Vietnam

\* Corresponding e-mail address: dinhhao@ntu.edu.vn

## ABSTRACT

**Purpose:** In this paper, the mechanical properties of welded joints of AA7075-T6 obtained using friction stir welding (FSW) with five regimes of ratio of tool rotation speed to weld speed (3.0, 4.0, 7.5, 10.0 and 15.0 rev/mm) are investigated.

**Design/methodology/approach:** FSW welds were fabricated by Friction stir welding machine. The properties of FSW and were identified using temperature and hardness distribution, microstructure, and tensile strength.

**Findings:** The weld heat and grain size rise when the ratio  $\omega/v$  or  $\omega$  is increased. Tensile strength of welded joint is increased when the ratio  $\omega/v$  is elevated. An FSW joint can be obtained with the highest tensile strength and strain of about 76% in comparison with that of the base metal. In all cases, tensile fractures take place outside the stirred zone and are locate in either the retreating or advancing side where hardness is the lowest.

**Research limitations/implications:** The paper researches about properties of FSW of AA7075-T6 that focus on tensile strength and some elements relation such as: temperature and hardness distribution, microstructure.

**Originality/value:** The results show that the mechanical properties of AA7075-T6 depended on friction stir welding parameters.

**Keywords:** Friction stir welding; Welding parameters; Microstructure; Hardness; Tensile strength

**Reference to this paper should be given in the following way:**

Duong Dinh Hao, Tran Hung Tra, Effects of friction stir welding parameters on the mechanical properties of AA7075-T6, Archives of Materials Science and Engineering 77/2 (2016) 58-64.

## PROPERTIES

### 1. Introduction

Aluminium alloy AA7075 is used extensively in aerospace industry with ultimate tensile strength about 572 MPa [1]. This is one of the aluminium alloys that is considered unsuitable for arc welding as with others in the AA2xxx series. These alloys are often used in high performance applications such as aircraft, aerospace and

competitive sport equipment of alloys. Therefore, the need to develop an advanced welding technology to overcome these weaknesses as well as improve strength at the weld is essential.

Friction stir welding (FSW) is now extensively used in aluminium industries for joining and material processing applications. This is a welding process in the solid state by the heat friction and application is mainly for non-ferrous

metals, especially aluminium and its alloys (Fig. 1) [2]. It is used particularly for joining aluminium alloys in shipbuilding and marine industries, aerospace, automotive and rail industries [3]. In comparison with fusion welding, the friction weld technique possesses several advantages such as high strength, free defects, low distortion, etc. [4].

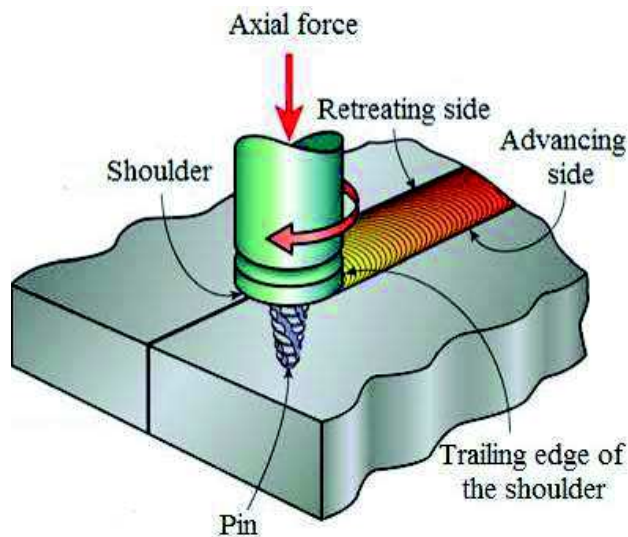


Fig. 1. Schematic diagram of friction stir welding [3]

These advantages are necessary for the developing aerospace industry as well as others fields. However, to broaden the application of FSW, the effect of the weld parameters on the properties of the joint need to be clarified. The aim of this study is to investigate the effect of tool rotation speed and weld speed on temperature and microstructure as well as the mechanical properties of the FSW butt-joints of AA7075-T6 plates.

Table 1.  
Chemical composition of AA7075-T6

| Element, | Al        | Zn      | Mg       | Cu    | Si      | Fe      | Mn      | Ti      | Cr        |
|----------|-----------|---------|----------|-------|---------|---------|---------|---------|-----------|
| %        | 87.1-91.4 | 5.1-6.1 | 2.11-2.9 | 1.2-2 | Max 0.4 | Max 0.5 | Max 0.3 | Max 0.2 | 0.18-0.28 |

Table 2.  
Mechanical and thermal properties of the base metal

| Material   | Ultimate tensile strength, MPa | Yield strength, MPa | Elongation, % | Hardness, Rockwell B | Modulus of elasticity, GPa | Poisson's ratio |
|------------|--------------------------------|---------------------|---------------|----------------------|----------------------------|-----------------|
| Base metal | 572                            | 503                 | 11            | 87                   | 71.7                       | 0.33            |

## 2. Experimental procedures

The 5.0 mm AA7075-T6 sheets, for which the chemical composition and mechanical showed in Table 1 and Table 2, respectively [1], were butt-joined by friction stir welding using. The tool geometry that was applied in this work was a scrolled shoulder tool and a truncated cone pin with a pin height of 4.8 mm, the pin diameter of 5.0 mm at the middle pin length, and a screw pitch of 1.0 mm. The pin was aligned at a tilt angle of 2.0 deg. in the plane describing the pin axis and the centre weld line (the tilt angle is defined as the angle between pin axis and the direction perpendicular to the workpieces). The tool tip was kept at a distance of 0.2 mm from the backing anvil. Various regimes of weld parameters were performed by varying the tool rotation speed (denoted  $\omega$ , revolving/min) and the weld speed (denoted  $v$ , mm/min).

During the welding, the weld heat input at the end weld centre and at the shoulder limit areas in advancing side or retreating side (1.0 mm far from the shoulder limit line) were measured by thermal couplings attached to the weld surface with a computer software interface (Fig. 2b). After welding, the samples were sectioned normal to the welding direction and then prepared by grinding disks, polished, and finally etched with a reagent: 150 mL H<sub>2</sub>O, 3 mL HNO<sub>3</sub>, 6 mL HCl, and 6 mL HF [5]. The microstructure was observed by Scanning Electron Microscope. The hardness in and around the welded zone was measured by a Rockwell machine with a ball indenter, 100 kg loading [6]. The tensile specimens were prepared according to ASTM E08 [7] by removing both the weld surface and the root surface layers of 1.5 mm thickness from the 5.0 mm FSW plate as shown in Fig. 3. The tensile strength of the FSW AA7075-T6 was measured by the 2.0 mm thickness plate specimens that were extracted in the perpendicular to the weld direction. The tensile tests were performed by an Instron machine 3366, 10 kN at a constant strain rate of 5.0 mm/min.

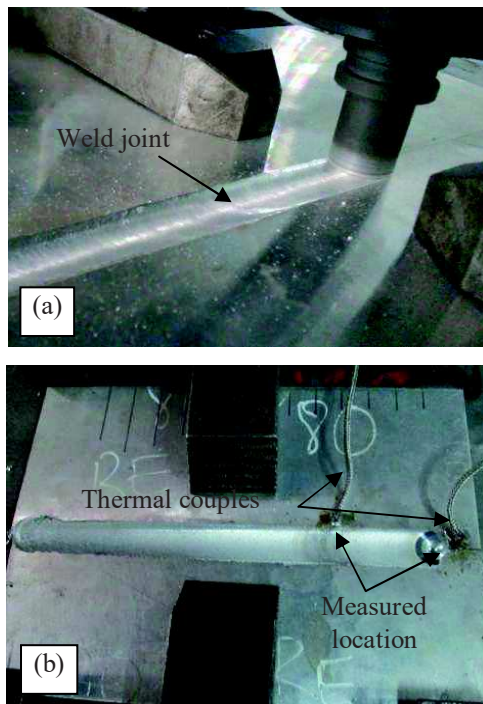


Fig. 2. Process of welding (a) and measuring temperature (b)

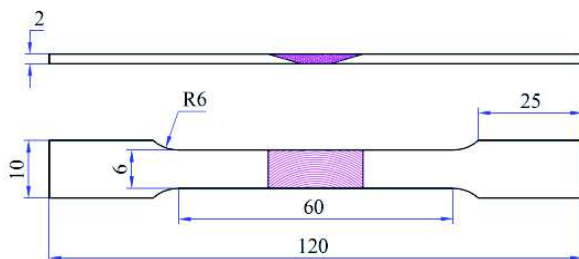


Fig. 3. Geometry of tensile specimen

### 3. Experimental results and discussion

#### 3.1. Temperature distribution

Determining temperature distribution within and around the stirred zone was important in explaining the mechanical properties of the welds. It influences directly the microstructure of the welds, such as grain size, grain boundary character, coarsening and dissolution of precipitates [8-11]. However, measuring temperature within the stirred zone is very difficult because of the intense plastic deformation produced by the rotation and translation of the pin tool. The results of weld temperature measured at the retreating side and at the end weld centre are shown in Figs. 4-5.

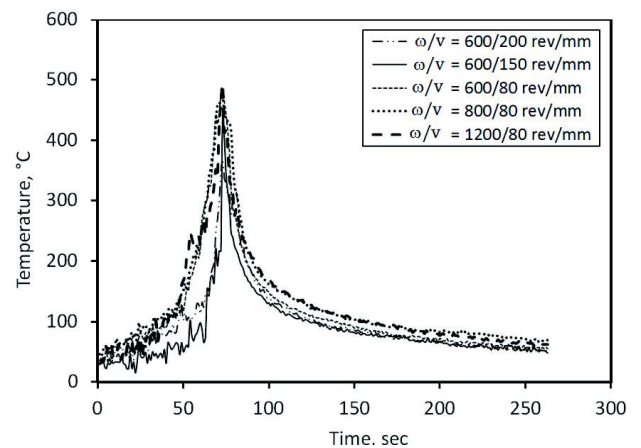


Fig. 4. Effect of weld parameters on the thermal cycle at the retreating side

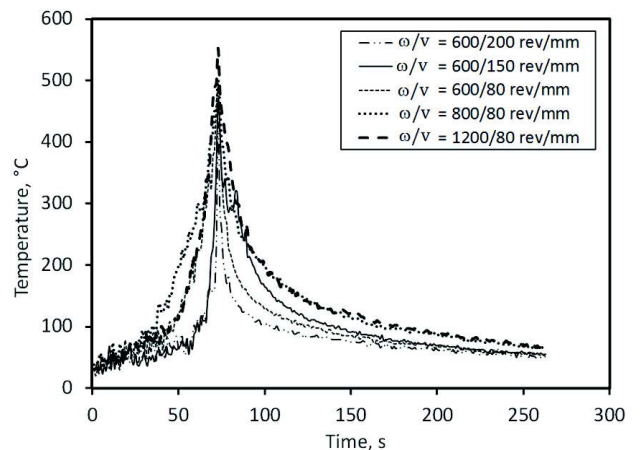


Fig. 5. Effect of weld parameters on the thermal cycle at the end weld centre

The dependence of the peak weld temperatures on rotation speed  $\omega$ , weld speed  $v$  and the ratio of rotation speed to weld speed  $\omega/v$  are shown in Fig. 6a, Fig. 6b and Fig. 7, respectively. Both rotation speed and weld speed influence peak weld temperature. It is shown that weld temperature increases with an increase in rotation speed and/or a decrease in weld speed. In all cases, maximum weld temperature was found at the weld center and this temperature was lower than the melting temperature of the base metal as is shown by the dash-lines. Furthermore, the results in Fig. 7 show that the peak weld temperatures are proportional to the ratio  $\omega/v$ . This increase can be generated by a combination of friction and plastic dissipation during deformation of the metal. Therefore, when the ratio of rotation speed to weld speed  $\omega/v$  decreases, the friction that

is created by the tool shoulder increased. Similarly, a change in rotation speed or weld speed also affected weld temperature.

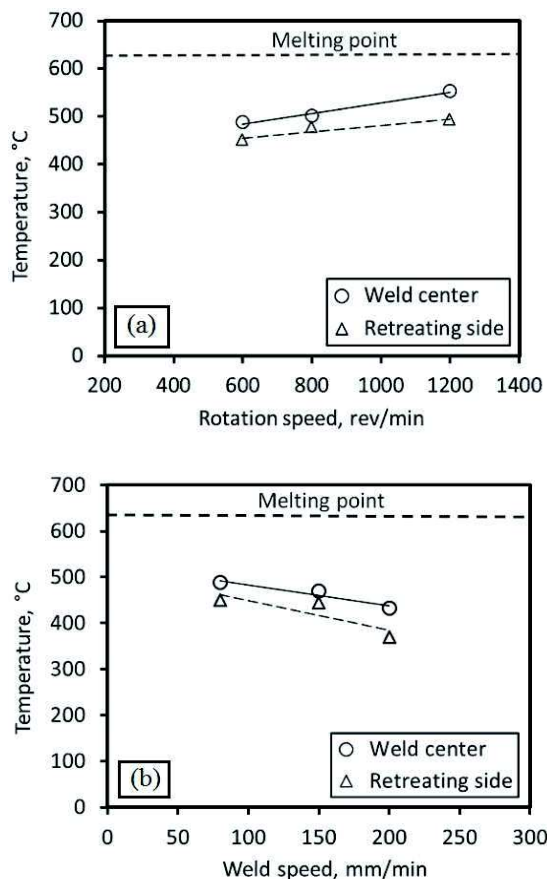


Fig. 6. Effect of rotation speed  $\omega$  at  $v = 80$  mm/min (a) and weld speed  $v$  on peak temperature at  $\omega = 600$  rev/min (b)

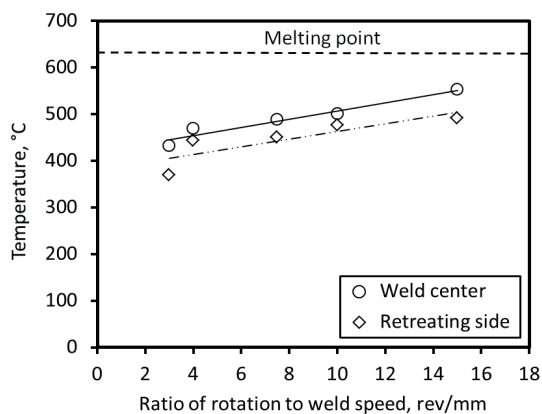


Fig. 7. Relation of peak weld temperatures with the ratio of tool rotation speed to weld speed ( $\omega/v$ )

After polishing, the welded microstructure was observed by naked eye and microscope, and some defects were found. These defects occurred in the regime  $\omega/v = 3.0$  and 15.0 rev/mm having a size of about 500  $\mu\text{m}$  (Fig. 8). From this view, it is reasonable to choose the ratio of tool rotation to weld speed,  $\omega/v$ , as a weld parameter covering both tool rotation speed and weld speed, and their interaction. The typical microstructure of a FSW AA7075-T6 when fabricated at  $\omega/v = 10.0$  rev/mm is characterized by the dynamic recrystallization was seen in Fig. 9. In general, grain size in the base metal where the material far enough from the center of the weld should not be affected by this process and were about 10-35  $\mu\text{m}$ , (region (IV) in Fig. 9d).

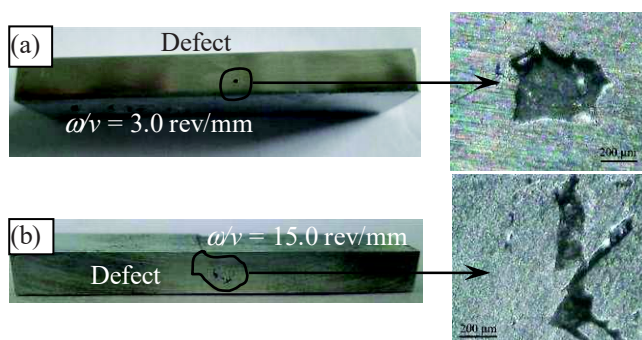


Fig. 8. The cross-sectional shape of the weld defect

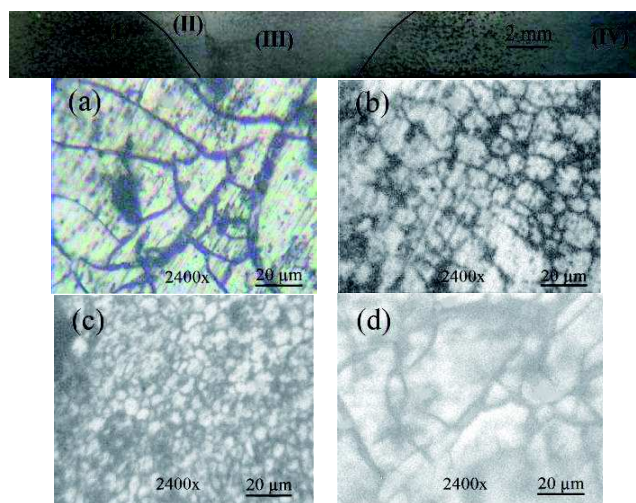


Fig. 9. Microstructure in the cross section of FSW at  $\omega/v = 10.0$  rev/mm, (a) region (I), (b) region (II), (c) region (III), and (d) base metal (IV)

Grain size in region (I) where the material has undergone a heat cycle without plastic deformation is the



same size as in the base metal (see region (I) in Fig. 9a). Region (II) where the material underwent plastic deformation due to the heating friction created by the shoulder tool, grain size appears to be finer than that in the zone (I). Grain size here are about 15-20  $\mu\text{m}$  (see region (II) in Fig. 9b). Finally, in the stir zone (III), material was the most severely deformed during soldering at the highest heat. Therefore, grain size is smallest compared with other regions about 5-8  $\mu\text{m}$  (see region (III) in Fig. 9c).

In addition, the experimental results also show that the grain size of the weld zone increased when the ratio of  $\omega/v$  rose (can see Fig. 10 and Fig.11). This elevation can be related to weld temperature effects on microstructural properties of friction stir welding.

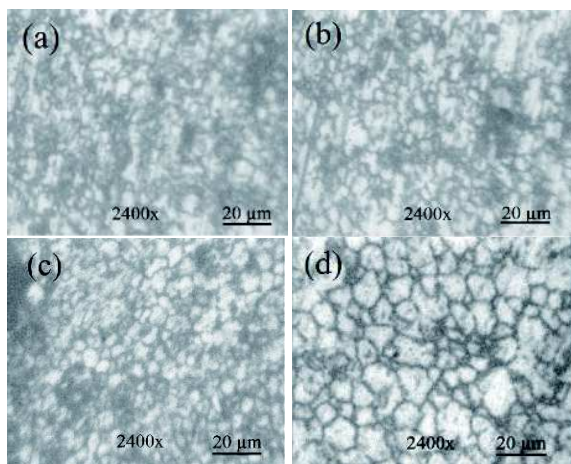


Fig. 10. Grain size of weld regimes in stirred zone, (a)  $\omega/v = 4.0$  rev/mm, (b)  $\omega/v = 7.5$  rev/mm, (c)  $\omega/v = 10.0$  rev/mm, (d)  $\omega/v = 15.0$  rev/mm

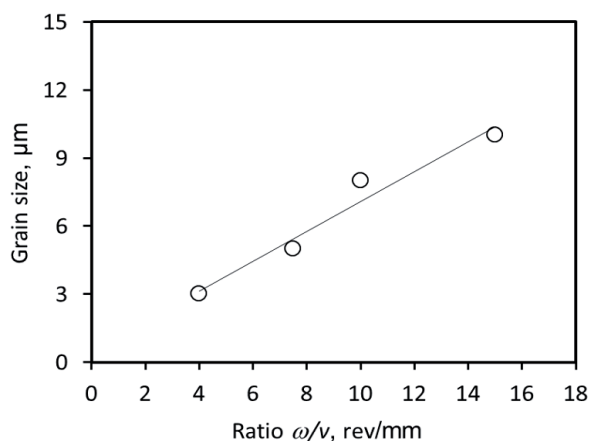


Fig.11. Effect of ratio of rotation speed to weld speed on grain sizes

### 3.2. Hardness distributions

Hardness distributions in the cross section of the FSW at  $\omega/v = 7.5$  rev/mm were investigated at location 1 and location 2 in Fig. 12. The results showed that the position of the minimum hardness is a heat-affected zone (HAZ). Hardness in the stirred zone is higher than in the HAZ but still lower than the base material (location away from the weld center). This may be related to the grain size of the welding zone. Hardness at location 1 is higher than at location 2 but being the difference is not statistically significantly. The hardness distributions measured at the middle-line in the cross sections are shown in Fig. 12 as a function of weld parameter,  $\omega/v$ .

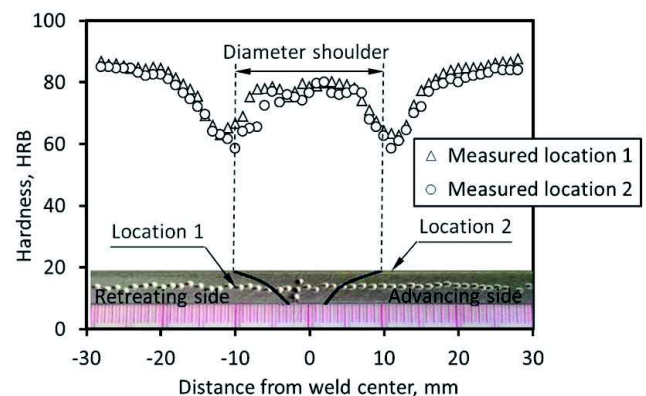


Fig. 12. Hardness in the cross section of the FSW at  $\omega/v = 7.5$  rev/mm

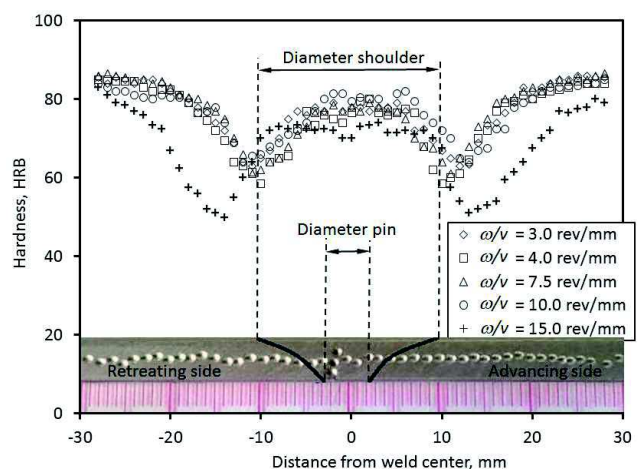


Fig. 13. Hardness distributions measured at the middle-line

In general, a softened area around the welded zone is observed in all FSWs. Here, the higher  $\omega/v$ , the higher weld

temperature (see Fig. 8) and the wider softened zone in the FSW (see Fig. 13). The width of the soft zone increases with an increase of  $\omega/v$ . The softening appearing in and around the welded zone could be related to the dissolution and/or coarsening of precipitates in this alloy [11]. It was also found, in all cases, that the lowest hardness in the cross section of the FSW is located in the heat affected zone (HAZ) in the advancing side and/or retreating side, outside the stirred zone. The fact that the hardness in the stirred zone is higher than that in HAZ might be associated with high density of grain boundaries in the stirred zone or Hall Petch effect [6].

### 3.3. Tensile strength

The tensile strength of the FSW of AA7075-T6 was investigated by an Instron machine at a constant strain rate of 5.0 mm/min. The results are shown in Fig. 3. The results show that the specimens in the regimes  $\omega/v = 3.0$  rev/mm and  $\omega/v = 15.0$  rev/mm were fractured at the stirred zone where microstructure of FSWs were defects that presented in Fig. 8. With these modes it can be seen that the weld quality was not satisfactory. The tensile failures of all remaining FSW specimens took place at the HAZ in the advancing side or in the retreating side as seen in Fig. 14.

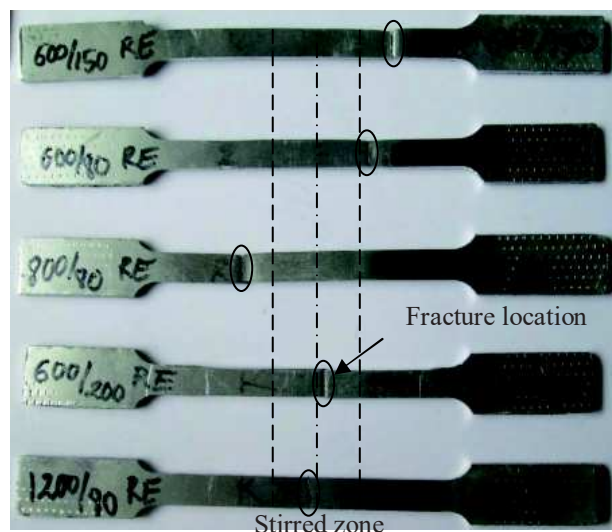


Fig. 14. Tensile fracture locations in the FSWs; the shoulder limits at the dash lines and weld centre at the dash-dot line

It should be noted that all tensile failures occurred outside the stirred zone. The tensile fracture locations were

well in agreement with the lowest hardness locations as seen in Fig. 13. This can be related to grain size in the welded zone.

Cross sections and tensile fracture locations in FSWs are presented in Fig. 15. Sliding planes and sliding direction of the samples that were destroyed inside and outside the welding zone were completely different. Sliding planes that occurred at stirred zone were always perpendicular to direction of axial force. This is demonstrated that the tensile failures were caused by only normal stress [6]. Fig. 14 also shown that the tensile specimen where  $\omega/v = 4.0$  rev/mm were necking before fracturing at the neck. The necking decreases as  $\omega/v$  increased from 4.0 to 10.0 rev/mm. This means that the length of the deformation decreases as  $\omega/v$  increases.

The stress-strain curves of the FSWs in different regimes are shown in Fig. 15, in comparison with that of base metal. The results of tensile strength and elongation under various weld conditions are presented in Fig. 16 and Fig. 17. In all weld conditions, the tensile property of the FSW was lower than that of base metal. Generally, the tensile strength and elongation of the FSWs were about 76% and 68% that of base metal, respectively. Here, the tensile strength increased when the weld parameter  $\omega/v$  was increased from 4.0 rev/mm to 10.0 rev/mm. This increase of tensile strength could be related to the higher heat input during the welding process as seen in Fig. 18, that must be result from the dissolution and/or coarsening of precipitates in and around the welded zone of this alloy.

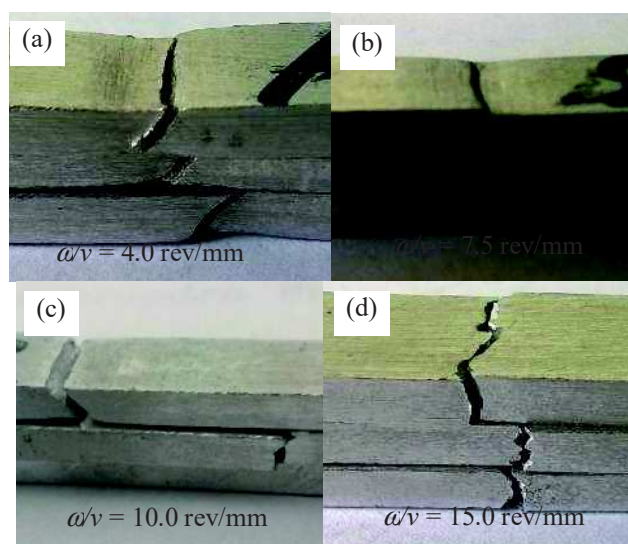


Fig. 15. Cross sections and the tensile fracture locations in FSWs at retreating side or advancing side (a-c), and stirred zone (d)

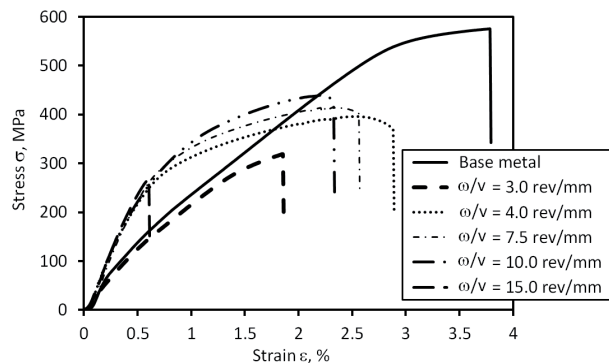


Fig. 16. Stress-strain curves of welded FSWs at weld modes

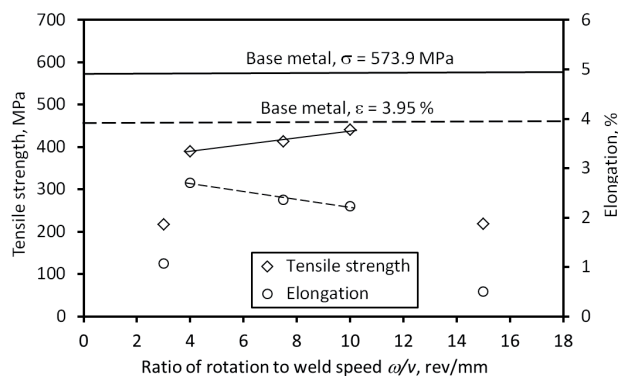


Fig. 17. Effect of ratio of rotation speed to weld speed on tensile strength and elongation

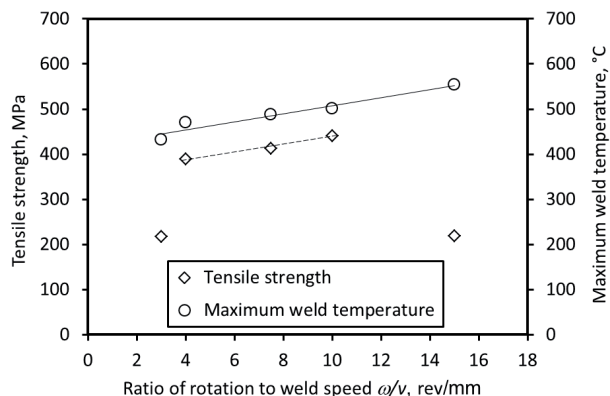


Fig. 18. Relation of tensile strength and weld temperature with the ratio of rotation speed to weld speed

#### 4. Conclusions

Friction stir welds of aluminum alloy 7075-T6 were successfully fabricated and the effects of weld parameters

on its thermal cycles, hardness, and tensile properties were investigated. The heat input was found to be proportional to the ratio of tool rotation speed to weld speed  $\omega/v$ . The joint is fabricated successfully when the ratio of rotational speed to weld speed  $\omega/v$  is in range from 4.0-10.0 rev/mm. The higher the ratio of rotation speed and weld speed, the higher tensile strength was but the lower elongation was. The highest tensile strength and elongation are about 76% and 68% compared with the base metal. The tensile fracture located outside the stirred zone, in the retreating side or advancing side, is where the hardness was lowest.

#### References

- [1] ASM Handbook. Volume 2: Properties and Selection: Nonferrous Alloys and Special-Purpose Materials, ASM International Handbook Committee, 1990, 450-462.
- [2] C.E.D. Rowe, W. Thomas, Advances in tooling materials for friction stir welding, TWI and Cedar Metals Ltd.
- [3] W.M. Thomas, I.M. Norris, D.G. Staines, E.R. Watts, Friction Stir Welding-Process Developments and Variant Techniques, Paper presented at SME Summit, Oconomowoc Milwaukee, USA, 2005.
- [4] R.S. Mishra, M.W. Mahoney, Friction Stir Welding and Processing, ASM International (2007) 1-5.
- [5] American Society for Metals, Metals Handbook 8<sup>th</sup> Edition, Metallography, Structures and Phase Diagrams, Vol. 8, 1973.
- [6] W.D. Callister, D.G. Rethwisch, Materials Science and Engineering 7th, John Wiley & Sons, Inc., 2007.
- [7] Standards ASTM, E08: Test Methods for Tension Testing of Metallic Materials, 2004.
- [8] D.P. Field, T.W. Nelson, Y. Hovanski, K.V. Jata, Heterogeneity of crystallographic texture in friction stir welds of aluminum, Metallurgical and Materials Transactions A: Physical Metallurgy and Materials Science 32/11 (2011) 2869-2877.
- [9] R.W. Ponda, J.F. Bingert, Precipitation and grain refinement in a 2195 Al friction stir weld, Metallurgical and Materials Transactions A: Physical Metallurgy and Materials Science 37 (2006) 3593-3604.
- [10] A. Oosterkamp, L.D. Oosterkamp, A. Nordeide, Kissing bond' phenomena in solid-state welds of aluminum alloys, Welding Journal 83/8 (2004) 225-231.
- [11] Y.S. Sato, H. Kokawa, M. Enomoto, S. Jogan, T. Hashimoto, Precipitation sequence in friction stir weld of 6063 aluminum during aging, Metallurgical and materials transactions A 30 (1999) 3125-3130.